PASJ: Publ. Astron. Soc. Japan **54**, 599–607, 2002 August 25

Superhump Evolution in the Ultrashort Period Dwarf Nova 1RXS J232953.9+062814

Makoto UEMURA,[1] Taichi KATO,[1] Ryoko ISHIOKA,[1] Hitoshi YAMAOKA,[2] Patrick SCHMEER,[3] Tom KRAJCI,[4] Donn R. STARKEY,[5] Ken'ichi TORII,[6] Nobuyuki KAWAI,[6,7] Yuji URATA,[6,8] Mitsuhiro KOHAMA,[6] Atsumasa YOSHIDA,[6,9] Kazuya AYANI,[10] Tetsuya KAWABATA,[10] Kenji TANABE,[11] Katsura MATSUMOTO,[12] Seiichiro KIYOTA,[13] Jochen PIETZ,[14] Tonny VANMUNSTER,[15] Arto OKSANEN,[16] and Antonio GIAMBERSIO[17]

[1]*Department of Astronomy, Faculty of Science, Kyoto University, Sakyo-ku, Kyoto 606-8502*
uemura@kusastro.kyoto-u.ac.jp
[2]*Faculty of Science, Kyushu University, Fukuoka 810-8560*
[3]*Bischmisheim, Am Probstbaum 10, 66132 Saarbrücken, Germany*
[4]*1688 Cross Bow Circle, Clovis, New Mexico 88101, USA*
[5]*AAVSO, 2507 County Road 60, Auburn, Auburn, Indiana 46706, USA*
[6]*Cosmic Radiation Laboratory, Institute of Physical and Chemical Research (RIKEN), 2-1, Hirosawa, Wako, Saitama 351-0198*
[7]*Department of Physics, Faculty of Science, Tokyo Institute of Technology, 2-12-1 Ookayama, Meguro-ku, Tokyo 152-8551*
[8]*Department of Physics, Science University of Tokyo, Kagurazaka, Shinjuku-ku, Tokyo 162-8601*
[9]*Department of Physics, Aoyama Gakuin University, 6-16-1, Chitosedai, Setagaya-ku, Tokyo 157-8572*
[10]*Bisei Astronomical Observatory, Ohkura, Bisei, Okayama 714-1411*
[11]*Department of Biosphere-Geosphere Systems, Faculty of Informatics, Okayama University of Science, Ridaicho 1-1, Okayama, Okayama 700-0005*
[12]*Graduate School of Natural Science and Technology, Okayama University, Okayama, Okayama 700-8530*
[13]*Variable Star Observers League in Japan (VSOLJ), Center for Balcony Astrophysics, 1-401-810 Azuma, Tsukuba, Ibaraki 305-0031*
[14]*Nollenweg 6, 65510 Idstein, Germany*
[15]*Center for Backyard Astrophysics (Belgium), Walhostraat 1A, B-3401, Landen, Belgium*
[16]*Nyrola Observatory, Jyvaskylan Sirius ry, Kyllikinkatu 1, FIN-40100 Jyvaskyla, Finland*
[17]*AAVSO, Via Rocco Scotellaro, 22 85100 Potenza, Italy*

(Received 2002 March 7; accepted 2002 June 19)

Abstract

We report on the evolution of superhumps and late superhumps in an ultrashort period dwarf nova, 1RXS J232953.9+062814, during the superoutburst in 2001 November. Ordinary superhumps were observed throughout a plateau phase, a rapid fading phase, and a rebrightening phase. During the plateau phase, the superhump period increased with time at a large rate of $P_{\rm dot} = 1.19 \pm 0.24 \times 10^{-4}$. In conjunction with the rebrightening phenomenon, these characteristics indicate that an accretion disk expanded further outward from the 3 : 1 resonance radius, which caused a large amount of left over matter at the outer disk, even after the superoutburst. In the post-outburst phase, we detected late superhumps superimposed on dominant double-peak modulations. Late superhumps were observed at least for 10 d without a significant period change. We detected the first normal outburst of this object on 2001 December 26. The interval between the superoutburst and this normal one is 53 d. This short recurrence time supports a high mass-transfer rate in this system. Concerning the evolutionary status of 1RXS J232953.9+062814, we propose that it is a progenitor of AM CVn stars on the evolutionary course of the cataclysmic variable channel in which systems have a secondary star with a hydrogen-exhausted core.

Key words: accretion, accretion disks — stars: binaries: close — stars: individual (1RXS J232953.9+062814)

1. Introduction

Cataclysmic variables (CVs) are semi-detached binaries which contain a white dwarf and a Roche-lobe filling secondary star (Warner 1995). The orbital-period distribution of hydrogen-rich CVs has some notable characteristics. One is a short-period cut-off at about 78 min, called the "period minimum". The other is a striking dearth between 2–3 hr, called the "period gap". They have been interpreted with the evolutionary scenario of CVs (Paczyński 1981; King 1988). The mass transfer in CVs is maintained by removal of the orbital angular momentum. The driving processes of angular-momentum loss have been believed to be gravitational-wave radiation and the magnetic braking (Taam et al. 1980; Rappaport et al. 1983). According to the standard evolutionary scenario based on these driving mechanisms, the period minimum is caused by a degeneracy of secondary stars, which leads to a system expansion with mass transfer. On the other hand, the period gap is caused by a disappearing of magnetic braking when secondary stars become fully convective at an orbital period of near 3 hr. This

Table 1. Details of the equipment used for photometric observations.

Site	Telescope	Camera	Filter
Kyoto	30 cm	ST-7E	unfiltered
Clovis	28 cm	CB245	unfiltered
Okayama	30 cm	ST-9E	unfiltered
Auburn	35 cm	ST-6B	V
Tsukuba	25 cm	AP-7	V, unfiltered
Ouda	60 cm	PixelVision SITe SI004AB	R_c
Idstein	20 cm	ST-6B	unfiltered
Wako	20 cm	AP-7p	unfiltered
Landen	35 cm	ST-7	unfiltered
Nyrola	40 cm	ST-7E	R_c
Bisei	30 cm	ST-8E	unfiltered
Potenza	20 cm	MX916	unfiltered

evolutionary model predicts a smaller mass-transfer rate in a system with a shorter orbital period, which has been confirmed by observations (Sproats et al. 1996).

Contrary to ordinary hydrogen-rich CVs, helium CVs, or AM CVn stars have ultrashort orbital periods of ~ 1000 s (Smak 1967; Warner, Robinson 1972; Nelemans et al. 2001). They are considered to have a secondary star of a helium white dwarf or a semi-degenerate helium star. For the formation of AM CVn stars, three models have been proposed: (1) the white-dwarf channel (Tutukov, Yungelson 1979), (2) the helium-star channel (Iben, Tutukov 1991), and (3) the CV channel (Podsiadlowski et al. 2001). The lack of possible progenitors of AM CVn stars has made it difficult to observationally determine which channels are real, or dominant.

Dwarf novae (DNe) form a subgroup of CVs. They experience repetitive outbursts with typical amplitudes of 2–5 mag (Warner 1987). Their outburst is considered to be a suddenly enhanced release of gravitational energy induced by a thermal instability of an accretion disk (Osaki 1996). According to the disk instability model, superoutbursts, which are observed only in SU UMa-type DNe, are induced by the tidal instability. The precession of a tidally distorted disk causes a beat phenomenon with the orbital motion of a secondary. It naturally explains superhumps, which are short-term modulations with a period slightly longer than the orbital period.

1RXS J232953.9+062814 is a recently discovered SU UMa-type DN (Uemura et al. 2001). Uemura et al. (2002, hearafter, Paper I) revealed extraordinary features that it has an ultrashort orbital period of ~ 64 min, although its optical spectrum is apparently hydrogen-rich. Its bright quiescent magnitude of $+7.8 < M_V < +8.8$, furthermore, indicates a high mass-transfer rate despite the short orbital period. This apparently contradicts the standard evolutionary scenario of ordinary hydrogen-rich CVs. Thorstensen et al. (2002) reported a conspicuous secondary star in this object, which is also quite atypical among short-period systems just above the period minimum. The evolutionary status and the driving mechanism of the mass transfer of this object are open issues.

In Paper I, we reported on the first results of our photometric campaign during the superoutburst in 2001 November. Here, we report on our detailed analysis of superhumps during the superoutburst and the post-outburst phase. In the next section, we show the evolution of superhumps with a brief description of our observation method. We then suggest an interpretation of the superhump evolution. We, furthermore, propose a possible evolutionary status of this object, in which it is a progenitor of AM CVn stars on the course of the CV channel. We summarize our findings in the final section.

2. Observation and Result

We performed CCD photometric observations at 12 sites. The equipment used in our observations is listed in table 1. We performed image reduction and an adjustment of each magnitude scale in the same manner as that mentioned in Paper I. The observation log is presented in table 2.

As reported in Paper I, the object experienced a superoutburst which was first detected on 2001 November 3 (HJD 2452217). Figure 1 shows the light curve during and after this superoutburst. The object entered a rapid fading phase on November 8 (HJD 2452221). A rebrightening subsequently occurred on November 9 (HJD 2452223). In this paper, we call a short period after rebrightening as a "transition phase", in which the decline rate decreased with time. The object then entered a post-outburst phase. No major brightening was observed until 2001 December 26 (HJD 2452269), when we detected another outburst, as can be seen in the right panel of figure 1. Throughout these phases, we detected periodic modulations whose period and profile varied with time. In the following subsections, we report on their detailed characteristics.

2.1. *Main Outburst and Rapid Fading Phase*

During the plateau of the superoutburst, we detected superhumps, as reported in Paper I. We estimated the observed peak times of the superhumps by taking cross-correlations between the average hump profile and observed light curves. Using these observed peak times, we obtained $O-C$s of each peak time (figure 2). In this figure, the average superhump period (0.046371 d) is indicated by the dotted line.

The $O-C$s during the plateau phase depict a smooth curve, and can be represented by a parabolic curve. We obtained a reduced χ^2 of 1.76 by fitting a parabolic function. This strongly indicates a significant increase of the superhump period. In SU UMa-type DNe, the period change of superhumps is a well-known phenomenon, from which we can obtain information about the evolution of a tidally distorted accretion disk. While most of them show the period decrease of superhumps, systems with quite short orbital periods tend to show the period increase of superhumps (Kato et al. 2001). Among short-period systems, it is important to note that the unique twin of 1RXS J232953.9+062814, V485 Cen also exhibited a period increase (Olech 1997). The rate of the period increase in V485 Cen is $P_{\rm dot}$ ($\equiv \dot{P}/P$) $= 2.8 \pm 0.3 \times 10^{-4}$, which is largest among known systems. By fitting a parabolic function to $O-C$s in figure 2, we estimated the rate of period change in 1RXS J232953.9+062814 to be $P_{\rm dot} = 1.19 \pm 0.24 \times 10^{-4}$. This is significantly smaller than that in V485 Cen and still larger than those in ordinary systems (Kato et al. 2001). In conjunction with an orbital period longer than that of V485 Cen,

Table 2. Journal of observations.

Date (HJD)	Time (hr)	T_{exp} (s)	N	Site*
2452217.9760	5.19	30	480	K
2452219.3652	1.91	40	163	L
2452219.4144	2.47	60	133	I
2452219.5782	2.45	80	100	A
2452219.9603	3.67	30	65	K
2452219.9871	4.02	70	188	T
2452220.6118	1.66	70	76	A
2452220.6766	2.47	20	238	W
2452220.9036	4.59	30	438	K
2452220.9106	4.57	15	219	T
2452221.3710	1.99	250	24	P
2452221.5638	2.36	80	100	A
2452221.9112	2.24	30	39	K
2452222.9532	1.15	30	31	K
2452223.2378	7.30	70	110	I
2452223.2379	6.34	50	145	L
2452223.7036	2.04	20	205	W
2452223.9062	6.17	40	507	B
2452224.0245	2.69	30	263	Ok
2452224.2167	6.35	70	126	I
2452224.2314	6.22	70	306	L
2452224.5011	2.09	90	80	A
2452224.8822	0.56	130	11	T
2452224.9391	2.94	30	56	K
2452225.2096	0.19	70	5	I
2452225.5099	2.31	120	67	A
2452225.6936	1.57	10	130	W
2452225.9039	3.12	30	164	K
2452225.9246	1.15	130	29	T
2452226.0141	1.13	30	110	Ok
2452226.5365	2.65	120	73	A
2452226.9849	4.76	30	166	K
2452227.4989	4.64	120	129	A
2452227.9028	6.78	30	631	K
2452228.3696	0.59	60	28	N
2452228.3914	1.85	90	52	I
2452228.8841	3.03	30	156	K
2452229.3500	2.32	90	84	I
2452229.8743	7.56	30	625	K
2452229.9192	2.85	130	78	T
2452229.9973	3.37	30	157	Ok
2452230.8758	7.46	30	313	K
2452231.0544	1.81	30	183	Ok
2452231.3236	2.73	60	138	N
2452231.5425	4.41	120	129	C
2452231.8788	5.50	30	293	K
2452232.0221	2.60	30	263	Ok
2452232.5461	3.41	120	100	C
2452232.8818	5.12	30	277	K
2452233.5314	3.57	120	83	A
2452233.5434	4.24	120	124	C
2452233.8881	6.36	30	581	K
2452234.5418	4.20	120	123	C
2452234.8685	7.24	30	701	K
2452235.0111	2.73	30	174	Ok
2452235.4864	3.03	150	71	A
2452235.5323	4.37	120	128	C
2452235.9906	3.10	45	212	Ok
2452237.9946	2.83	45	77	Ok
2452238.0044	3.81	30	260	K
2452238.5221	4.06	120	119	C
2452238.9492	4.61	30	320	K
2452239.8934	0.84	30	60	K
2452239.9454	1.74	70	85	T
2452240.5243	4.20	120	123	C
2452240.8716	6.01	30	575	K
2452241.9554	3.55	30	253	K
2452241.9857	2.38	45	68	Ok
2452242.5424	3.65	120	107	C
2452243.8809	6.20	30	280	K
2452244.8868	5.26	30	383	K
2452245.5260	3.41	120	100	C
2452245.9123	4.51	30	352	K
2452247.5261	2.00	120	59	C
2452247.9110	5.41	30	435	K
2452250.0096	2.14	30	201	K
2452250.8629	5.68	30	511	K
2452251.8875	2.56	30	177	K
2452252.5287	3.31	120	97	C
2452253.5268	3.31	120	97	C
2452254.9825	2.35	30	169	K
2452255.9531	4.14	45	163	Ok
2452256.9783	3.53	45	47	Ok
2452257.0608	0.92	30	37	K
2452257.5244	3.10	120	91	C
2452257.9634	3.89	45	85	Ok
2452258.0030	1.88	30	149	K
2452258.9022	5.36	45	218	Ok
2452258.9026	6.51	30	205	K
2452259.9276	4.81	30	314	K
2452260.9438	2.87	30	140	K
2452261.5302	2.65	120	78	C
2452261.9082	2.99	45	83	Ok
2452261.9165	2.08	30	49	K
2452262.5225	2.76	120	81	C
2452262.8798	0.12	10	25	Ou
2452262.9076	5.90	30	544	K
2452263.5265	2.62	120	77	C
2452263.9006	2.89	30	272	K
2452266.5227	2.50	120	74	C
2452266.8700	6.36	30	550	K
2452267.8857	4.68	30	319	K
2452268.5245	2.31	120	68	C
2452269.8683	2.82	10	534	Ou
2452269.9447	3.86	30	346	K
2452270.5190	2.33	60	132	C
2452270.8552	1.70	10	264	Ou
2452270.9246	3.78	30	337	K
2452271.5213	2.20	120	65	C
2452271.8612	1.75	10	153	Ou

Table 2. (Continued)

Date (HJD)	Time (hr)	$T_{\rm exp}$ (s)	N	Site*
2452272.8588	0.11	10	28	Ou
2452277.9385	1.59	30	162	K
2452282.9212	0.67	30	69	K
2452286.8866	0.18	30	19	K
2452286.8866	0.18	30	19	K
2452293.8885	1.93	30	189	K
2452298.8972	1.36	30	132	K
2452301.9210	0.33	30	29	K
2452303.8964	0.92	30	82	K

* K = Kyoto, T = Tsukuba, C = Clovis, N = Nyrola, Ou = Ouda, I = Idstein, B = Bisei, A = Auburn, Ok = Okayama, W = Wako, L = Landen, P = Potenza.

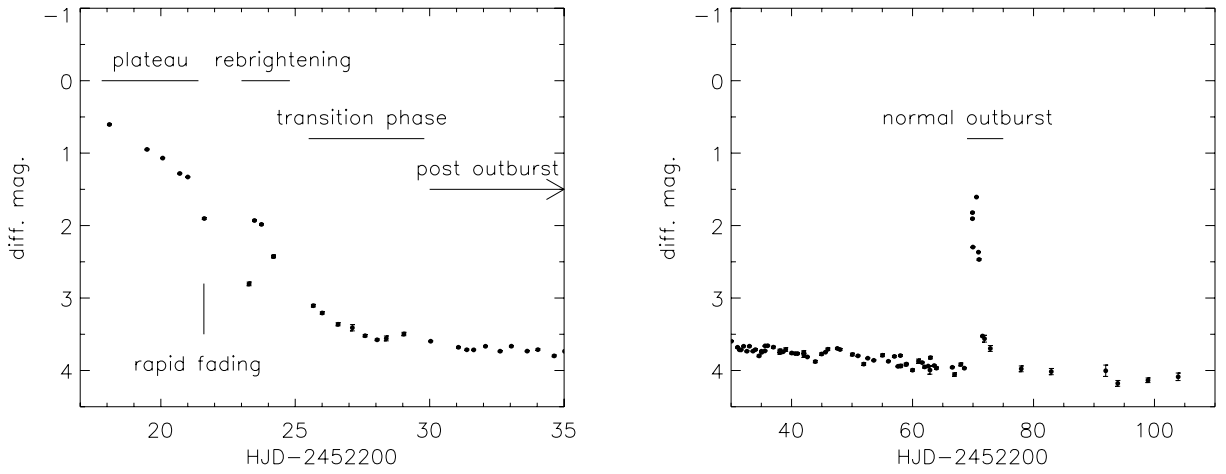

Fig. 1. Light curves of 1RXS J232953.9+062814 during and after the outburst in 2001 November. The abscissa and ordinate denote HJD and the differential magnitude, respectively. The filled circles represent the averaged magnitudes during each night. Left panel: Light curve including the superoutburst. We define four phases during this period, as shown in the panel (see the text). Right panel: Light curve during the post-outburst phase including a normal outburst.

the object thus lies between V485 Cen and ordinary short-period systems in the $P_{\rm dot}$–$P_{\rm SH}$ diagram (see, figure 10 of Kato et al. 2001).

We detected periodic modulations even in the rapid fading phase, as shown in figure 3. The humps had a single-peak profile and a period analogous to that of superhumps. In most SU UMa stars, superhump signals generally weaken in the late stage of superoutbursts and almost disappear in the rapid fading phase. Instead of ordinary superhumps, other types of modulations, called late superhumps generally appear (Haefner et al. 1979; Vogt 1983). While they have the superhump period, their peak shifts by about 0.5 phase shifted from that of ordinary superhumps. Using the average light curve of superhumps in the plateau phase, we estimate two peak times of the humps in figure 3, which are plotted in figure 2. The phase of these peak times roughly coincides with that of superhumps before the rapid fading phase. This indicates that the humps in the rapid fading phase are not late superhumps, but ordinary superhumps. Their amplitudes are about 0.15 mag, which are comparable to those just before the rapid fading phase. This is atypical for ordinary superoutbursts, and implies that the effect of tidal dissipation was still efficient even in this stage.

The $O-C$ diagram shows that the hump peaks during the rapid fading phase lie slightly earlier than that expected from the constant period increase indicated by a solid curve. When we fitted a parabolic function using the $O-C$s including these two points, it yielded a reduced χ^2 of 2.78. Compared with that

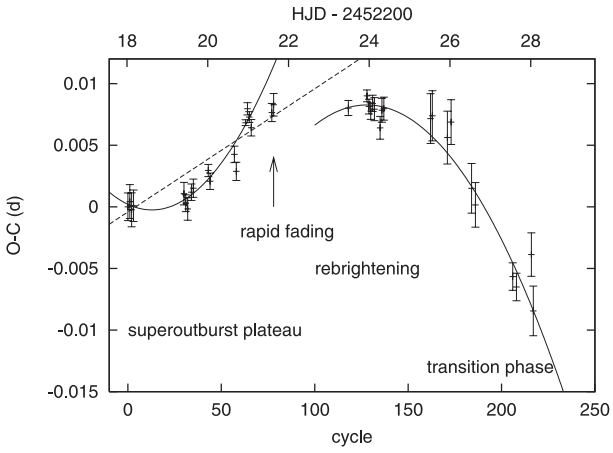

Fig. 2. $O-C$ diagram of superhumps through the main plateau, rapid fading, rebrightening, and transition phase. The abscissa denotes the cycle. We also show the corresponding HJD at the upper axis. The ordinate denotes $O-C$ (d). We calculated the $O-C$s from peak times of humps ($T_{\rm peak}$) determined by $T_{\rm peak}$ = HJD 2452218.02058 + 0.046271E, where E is the cycle. The dotted curve indicates an average superhump period of 0.046371 d. We calculated $O-C$s in this figure with a period 0.0001 d shorter than the average superhump period in order to clearly show period changes. The solid lines indicate parabolic curves fitted to the $O-C$s (see the text).

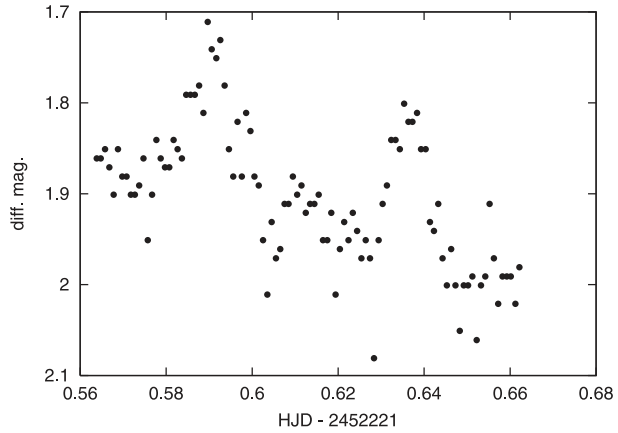

Fig. 3. Light curve during the rapid fading phase including two humps. The abscissa and ordinate denote HJD−2452221 and the differential magnitude, respectively.

calculated using the points without them, this result indicates that the period increase is significantly weakened in the rapid fading phase.

2.2. *Rebrightening*

The light curves during rebrightening are shown in figure 4. The beginning of rebrightening was detected 1.6 d after the rapid fading phase. The object reached the maximum of rebrightening between HJD 2452223.55 and 2452223.70, within only two days from the rapid fading phase. The rebrightening phenomenon after a superoutburst is frequently observed in SU UMa-type DNe with short orbital periods (e.g. Kato et al. 1997). The interval between the main superoutburst and the rebrightening is, however, quite short in the case of this system. Even in the case of V485 Cen, Olech (1997) reported that the object reached the peak of a rebrightening 4–6 d after a rapid fading phase.

As can be seen in figure 4, periodic modulations still appeared in both ascending and descending branches of the rebrightening. The amplitude of these humps was 0.10–0.15 mag and slightly increased with time. We calculated $O-C$s of these humps in the same way as mentioned above, and show them in figure 2. While we can see $O-C$s during rebrightening almost equal to those in the rapid fading phase, it is not evident that superhumps appeared throughout these phases without any period shifts, because of the lack of observations between these phases. On the descending branch of rebrightening, the second hump rapidly evolved, as can be seen in figure 4. In an ordinary SU UMa-type DNe, a rapid growth of late superhumps is frequently observed in the late plateau phase of superoutbursts. The evolution of hump profiles in figure 4 is reminiscent of that phase. We hence suggest that the main humps and the second humps in the rebrightening phase are superhumps and late superhumps, respectively.

2.3. *Transition and Post-Outburst Phase*

The rapid fading from the rebrightening lasted for at least 0.8 d, and then the fading became gradual at $\sim 0.01\,\mathrm{mag\,d^{-1}}$ after the transition phase, which was lasted for ~ 5 d. The fading rate decreased with time during the transition phase. We show

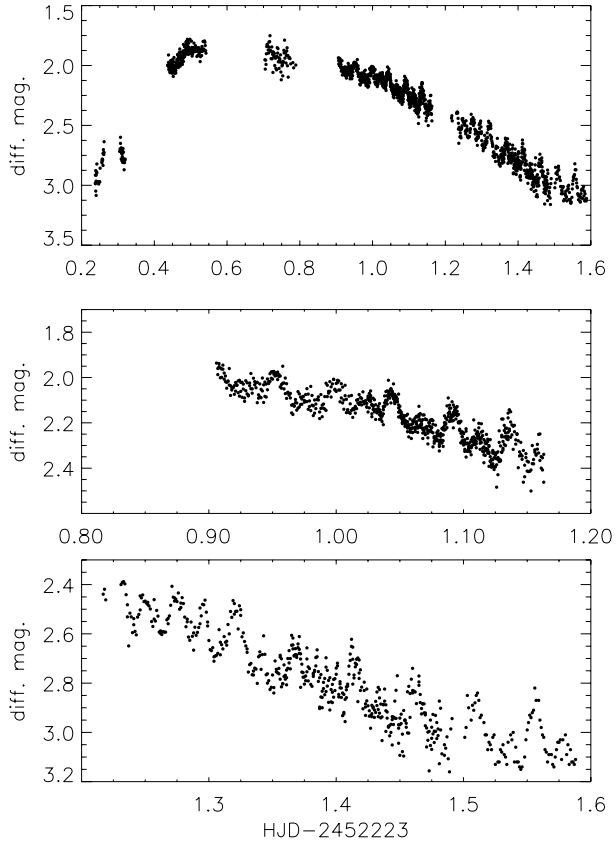

Fig. 4. Light curves around rebrightening. The abscissa and ordinate denote HJD−2452223 and the differential magnitude, respectively. Top panel: Light curve of all rebrightening. Middle and bottom panels: Light curve between HJD 2452223.8–2452224.6. The horizontal and vertical scales are the same in order to compare them clearly.

representative light curves during these phases in figure 5.

As can be seen in the right panel of figure 1, the long-term light curve of the post-outburst phase can be described by gradual fading with a minor reflare. The minor flare occurred in HJD 2452247 with an amplitude of ~ 0.20 mag. Although it only has small amplitudes, independent confirmations by observations at Kyoto and Clovis support that it is a real event. On the other hand, larger variations after $\sim$ HJD 2452255 are mainly caused by a bad seasonal condition. This small amplitude reflare is different from rebrightening regarding a lack of rapid fading. After relatively gradual brightening, the object started fading at a rate comparable to that before the minor flare, as can be seen in the right panel of figure 1.

The nature of dominant short-term modulations changed during the transition phase. As can be seen in figure 5, superhumps were still prominent and had more evolved second humps in the early transition phase. The profile then became more complicated in the late transition phase. To calculate the peak times of the humps, we divided the light curve into two-day bins and made their average light curves. Cross-correlations between the average and observed light curves yielded $O-C$s of the humps, which are shown in figure 2. This figure includes no hump in the late transition phase, since the complicated profile makes it difficult to determine the peak

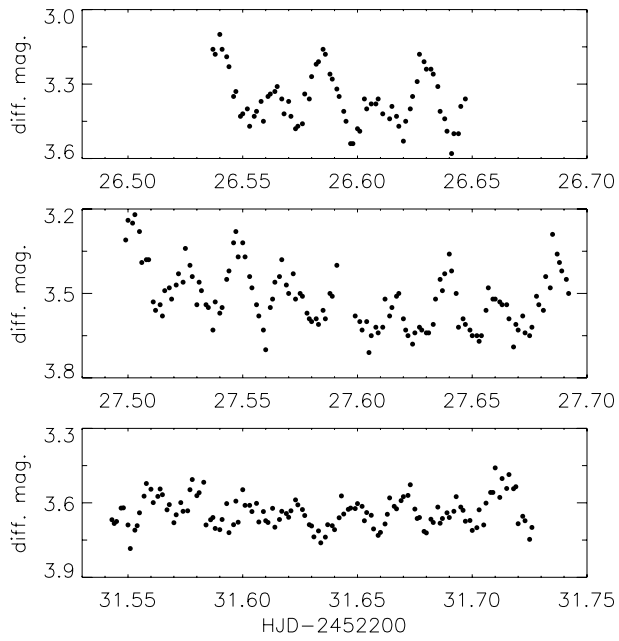

Fig. 5. Light curves for the transition and the post-outburst phases. The abscissa and ordinate denote HJD−2452200 and the differential magnitude, respectively. The panels show examples of short-term variations in the transition phase (HJD 2452226 and 2452227) and in the post-outburst phase (HJD 2452231).

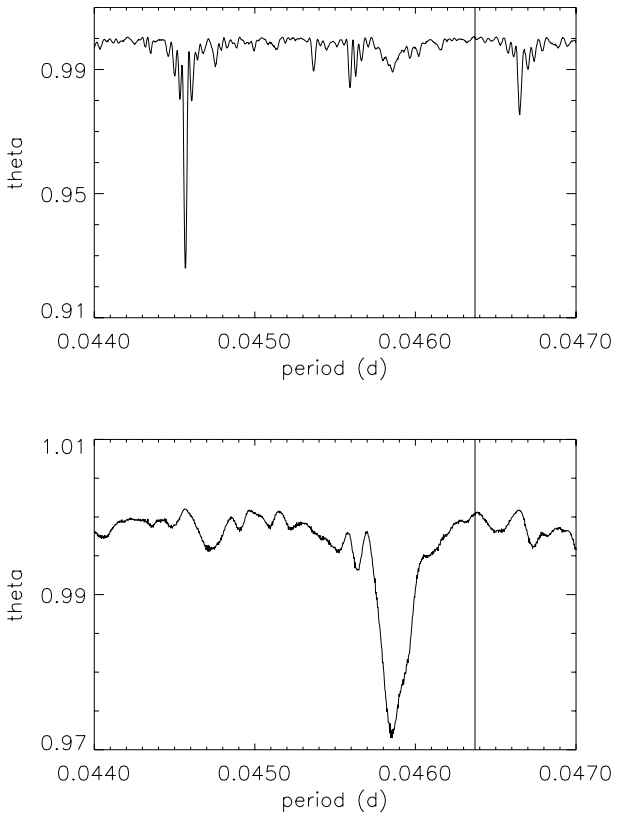

Fig. 6. Period–Θ diagrams calculated from the light curve during the post-outburst phase. The abscissa and ordinate denote the period in days and the theta, respectively. Top panel: Period–Θ diagram of the double-peak modulations which dominate in the post-outburst phase. Lower panel: Period–Θ diagram of the residual light curve. The vertical lines appeared in both panels indicate the superhump period during the plateau phase (0.046371 d).

times. As can be seen in figure 2, the $O-C$s in the rebrightening and transition phases depict a smooth curve. This systematic period shift from the rebrightening phase strongly indicates that superhumps appeared at least until the early transition phase. Using all points during the rebrightening and transition phases in figure 2, fitting a parabolic function yielded $\chi^2 = 1.19$ and $P_{\rm dot} = -9.15 \pm 1.86 \times 10^{-5}$. We show the fitted curve in figure 2 by a solid line. As can be seen from this figure and the fitted curve, it may be possible that the period shift had already stopped during the mid-transition phase (cycle ~ 200). In this case, we obtained $P_{\rm dot} = -8.22 \pm 3.34 \times 10^{-5}$ from a χ^2 fitting without the points of a cycle > 200 in figure 2. While these $P_{\rm dot}$ are relatively large, they are rather normal among ordinary SU UMa-type DNe (Kato et al. 2001). The $O-C$s in the rapid fading phase are apparently not on this curve of the constant-period decrease.

In the post-outburst phase, the light curve was dominated by double-peak modulations, whose amplitude was slightly variable. The typical light curve is shown in the bottom panel of figure 5. In Paper I, we performed a period analysis using the light curve for the first three days in the post-outburst phase. This revealed that the double-peak modulations have a period significantly shorter than the superhump period. Thorstensen et al. (2002) have recently revealed that, in conjunction with the spectroscopic phase, the photometric modulations are ellipsoidal modulations caused by the orbital motion of a tidally distorted secondary. To obtain a more accurate photometric period, we analyzed the light curve during the post-outburst phase from HJD 2452230 to 2452271. When we calculated the period, observations during the normal outburst were excluded, except for that on HJD 2452271.50–1.65 in which the double-peak modulations had already appeared (see the next subsection). After subtracting the slow fading trend and the minor reflare profile, we performed a period analysis with the phase dispersion minimization method (PDM; Stellingwerf 1978), which yielded the period–Θ diagram shown in the upper panel of figure 6. In this figure, we indicate the superhump period with a solid line. We can see a strong periodicity shorter than the superhump period. A weak signal slightly longer than the superhump period is the one-day alias of this strong signal. We determined the period to be 0.0445652 ± 0.0000007 d. This photometric period is almost equal to a spectroscopic period reported by Thorstensen et al. (2002).

Although double-peak modulations dominate in the post-outburst phase, their variable amplitude implies another periodicity. We subtracted the average profile of the double-peak modulations from the light curve and performed a PDM analysis with the residual light curve. The obtained period–Θ diagram is shown in the lower panel of figure 6. There is a strong periodicity which is longer than that of double-peak modulations and shorter than the average superhump period. We determined the period to be 0.045855 ± 0.000010 d. The average light curve of residual modulations is shown in figure 7. It has a single-peak profile with the amplitude of ~ 0.05 mag. The

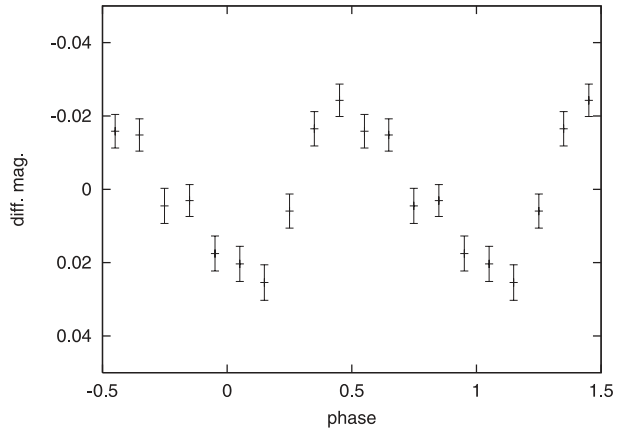

Fig. 7. Average light curve of late superhumps. The abscissa denotes the phase in the late superhump period. The ordinate denotes the differential magnitude, whose scale is adjusted by subtracting the average magnitude.

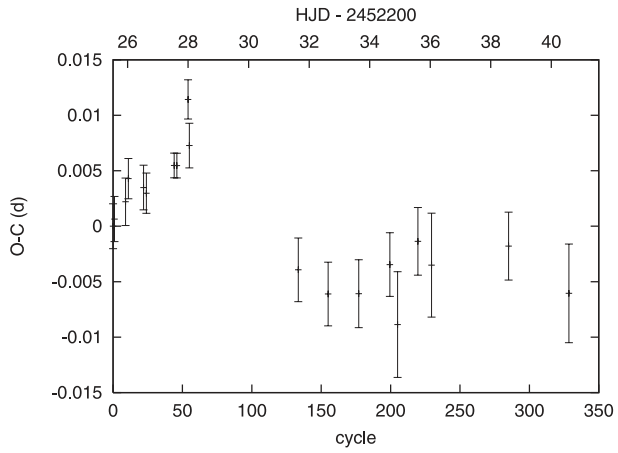

Fig. 8. $O-C$ diagram of superhumps during the transition and post-outburst phases. The abscissa and ordinate denote the cycle and the $O-C$ (d), respectively. $O-C$s in this figure were calculated with the period of the residual modulations in the post-outburst phase, i.e., $T_{\rm peak}$ = HJD 2452225.523642 + 0.045855E.

humps were constant in amplitude for at least 10 d.

We calculated the peak times of residual humps with their average light curve. Their $O-C$s determined with the period of residual modulations are shown in figure 8. This figure also includes a part of $O-C$s in the transition phase. Figure 8 reveals that the residual modulation has characteristics different from that in the early transition phase. First, we can find no significant period change over 200 cycles. The period of residual modulations was thus constant or variable with only a small $P_{\rm dot}$. Second, their peak timings are apparently shifted compared with those in the transition phase. The peak time of residual modulations is rather near that of second humps evolving through the rebrightening–transition phase. In conjunction with their long-lived nature and single-peak profile, we conclude that the residual modulations are late superhumps and that ordinary superhumps disappeared during the transition phase.

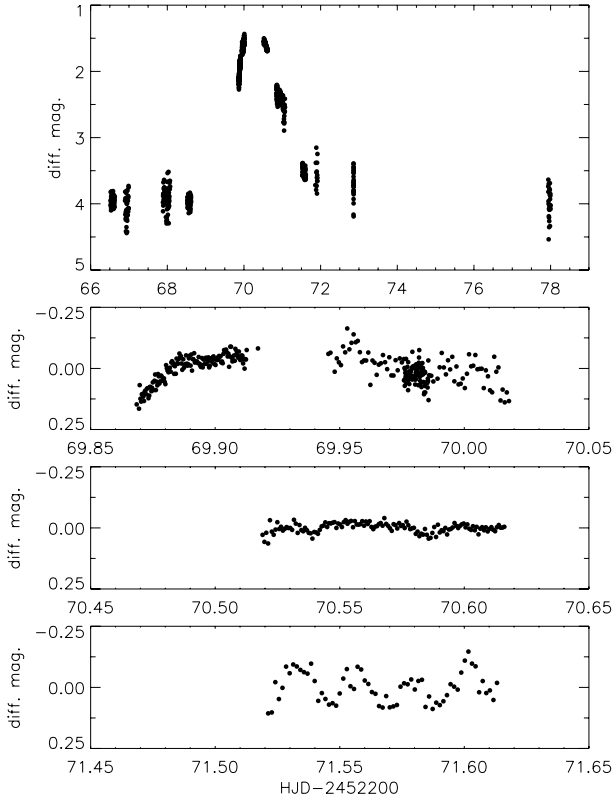

Fig. 9. Light curves during the normal outburst. The abscissa and ordinate denote HJD−2452200 and the differential magnitude, respectively. Top panel: Long-range light curve during the normal outburst. Lower three panels: Short-range light curves during the rising stage (HJD 2452269–70), the early fading stage (HJD 2452270), and the late fading stage (HJD 2452271). Each light curve is subtracted the linear rising or fading trend.

2.4. *Normal Outburst*

We detected another outburst in HJD 2452269. We show the light curve of this outburst in figure 9. A rapid brightening was successfully detected in the late HJD 2452269. The rising rate decreased with time from 7.6 mag d^{-1} to 2.3 mag d^{-1} during this run. The observed maximum was 1.1 mag fainter than the supermaximum in 2001 November. The object then started rapid fading at a rate of 1.6 mag d^{-1}. The fading became more gradual near the quiescent level.

Short-term modulations weakened in amplitude during this outburst. While we can see some hints of modulations during the rising stage, our period analysis provided no significant periodicity. On the other hand, modulations during the early fading stage are relatively evident, as shown in figure 9. Our observation detected two dip-like profiles whose amplitudes were 0.04 mag. We estimated the separation between the two dips to be ~ 0.046 d, which is reminiscent of the orbital or superhump period. Folding the light curve with the photometric orbital period of 0.0445652 d, we found that the phase of these dips corresponds to the phase of a minimum of double-peak modulations. This strongly indicates that the dips are signals associated with the orbital motion. In the late fading stage, the light curves were dominated by double-peak modulations as

seen in the bottom panel of figure 9. After this outburst, the object again started gradual fading, as shown in figure 1. The object became ~ 1 mag fainter during the post-outburst phase for 70 d. The amplitude of the superoutburst is hence ~ 4 mag.

The lack of superhumps and the short duration (~ 2 d) of the outburst are evidence that the outburst is a normal one. This is the first normal outburst confirmed after the object was classified as an SU UMa-type DN. The interval between the superoutburst and the normal outburst is 53 d. This recurrence time is quite short among short-period SU UMa stars and rather analogous to long-period SU UMa stars having orbital periods near 2 hr (Warner 1995).

3. Discussion

3.1. Interpretation of the $O-C$ Diagram

The ordinary period decrease of superhumps has been attributed to decreasing apsidal motion due to a shrinking disk during superoutbursts (Warner 1985; Patterson et al. 1993). On the other hand, the period increase of superhumps is proposed to be the result of an expanding disk beyond the 3 : 1 resonance radius (Kato et al. 1997; Kato et al. 2001). In this scenario, the eccentricity wave can propagate outward when a system has a large amount of accumulated matter due to a small mass-transfer rate ($\dot{M}$) and/or has a small 3 : 1 resonance radius due to a small mass ratio ($q \equiv M_2/M_1$).

In Paper I, we suggested an unexpectedly high $\dot{M}$ in 1RXS J232953.9+062814 based on a bright absolute magnitude at quiescence. In this paper, we have furthermore revealed that the recurrence time between the superoutburst and the normal one is quite short among short-period systems. According to the disk instability model (Osaki 1995), this short recurrence time also supports a high $\dot{M}$.

It is thus less likely that the period increase in 1RXS J232953.9+062814 is caused by a small $\dot{M}$. It is, however, also problematic to explain it with a small q. In Paper I, we suggest a secondary star with relatively large mass based on a large superhump excess and high effective temperature of the secondary (see also Thorstensen et al. 2002). This provides a relatively large q of 0.19 ± 0.02 while short-period systems are expected to have $q \sim 0.05$.

Additionally to the period increase of superhumps, the post-outburst rebrightening phenomenon is also analogous to ordinary short-period systems. Osaki et al. (1997) proposed a model that the rebrightening is caused by a temporal increase in viscosity at a cold state. In short-period systems, a large amount of accumulated matter enables a disk to expand further outward. The left over matter can re-ignite after the superoutburst when the magnetic field, or viscosity gradually decays (Osaki et al. 2001).

On the other hand, the outer portion of the disk can be a superhump light source propagating outward, which leads to the period increase of superhumps (Kato et al. 1997). This scenario indicates that a large amount of left over matter can cause both the period increase of superhumps and the rebrightening phenomenon. The detection of rebrightening in 1RXS J232953.9+062814 may support that its period increase of superhumps was also caused by a large amount of left over matter. We detected superhumps even in the rapid fading phase and the rebrightening phase without any noticeable decreasing in the amplitude. This also indicates the presence of a large amount of matter at the outer disk, in which the tidal dissipation was still efficient even after the superoutburst. Since the object has a large q and $\dot{M}$, additional unknown mechanisms are needed to expand a disk further outward from the 3 : 1 resonance radius.

While the superhump period started decreasing in the rapid fading phase, a constant decreasing rate cannot explain the subsequent period decrease in the rebrightening and the transition phase, as shown in figure 2. It is possible that the superhump period had continuously decreased from the rapid fading phase to the transition phase at variable rates of the period decreasing. The disk instability model, however, rather prefers a scenario that the rapid period decrease after the superoutburst was interrupted by the expansion of the disk, or the period increase during the rising stage of rebrightening.

Superhumps rapidly disappeared during the late transition phase, as shown in figure 5. When double-peak modulations and late superhumps subsequently became dominant, the period change had already stopped, as can be seen in figure 8. Late superhumps have been proposed to be caused by the brightness variation of the stream–disk impact region (Haefner et al. 1979; Vogt 1983). Based on this model, we consider that the tidal dissipation was no longer significant in the late transition phase, while the disk was still eccentric. The gradual fading trend during the post-outburst phase was possibly associated with the gradual decay of the eccentricity of the disk. Such a long, fading tail is frequently observed in WZ Sge-type DNe, although they have a small q compared with 1RXS J232953.9+062814.

3.2. Evolutionary Status of 1RXS J232953.9+062814

As noticed in Paper I, this object apparently breaks the standard scenario of CV evolution regarding its ultrashort orbital period despite the high $\dot{M}$, the large q, and the hydrogen-rich spectrum. The proposed q of 0.19 ± 0.02 in Paper I indicates a secondary star more massive than that in short-period SU UMa stars. A massive secondary star can be consistent with the high $\dot{M}$ when we consider gravitational-wave radiation to be a process of angular-momentum removal from the system.

The ordinary evolutionary sequence of CVs has been considered with secondary stars near main-sequence stars (e.g. King 1988). This sequence makes the period minimum around 70 min and is difficult to explain the presence of 1RXS J232953.9+062814. We propose that this object has an evolved secondary star which has a hydrogen-exhausted core (see also Thorstensen et al. 2002). A secondary star with a hydrogen-exhausted core has mass more than that expected from the mass–radius relation of main-sequence stars and brown dwarfs. According to Podsiadlowski et al. (2001), such systems have a shorter period minimum and, furthermore, have more luminous secondary stars around their period minimum. They predicted that, before the period minimum, such CVs still have much hydrogen in their surface, which is consistent with the hydrogen-rich spectrum of 1RXS J232953.9+062814.

To perform a rough estimate of the $\dot{M}$ of the object, we assumed the masses of a white dwarf and a secondary star to

be $M_1 = 0.7\,M_\odot$ and $M_2 = 0.14\,M_\odot$, respectively. In conjunction with an orbital period of 64 min, we estimated the rate of angular-momentum loss due to gravitational-wave radiation ($\dot{J}_{\rm GR}$) to be about 7-times larger than that of ordinary short-period systems ($M_1 = 0.7$, $M_2 = 0.065$, and $P_{\rm orb} = 80$ min assumed). We need a mass–radius relation of secondary stars to translate $\dot{J}$ into $\dot{M}$. If we assume the empirical relation of ordinary CVs, $\dot{M}$ of the object is about 9-times larger than that of ordinary short-period systems.

Theoretical calculations show that CVs having secondary stars with hydrogen-exhausted cores evolve without a fully convective phase until secondary stars degenerate (Baraffe, Kolb 2000; Podsiadlowski et al. 2001). In these systems, we can hence expect the effect of magnetic braking even for orbital periods shorter than 2 hours. We estimated the rate of angular-momentum loss due to magnetic braking ($\dot{J}_{\rm MB}$) based on Rappaport et al. (1983). The system parameters of 1RXS J232953.9+062814 yield $\dot{J}_{\rm MB}$ 60% larger than $\dot{J}_{\rm GR}$. We calculated the total $\dot{M}$ of an object 24-times larger than that of ordinary short-period systems assuming the empirical mass–radius relation. This large $\dot{M}$ can explain the quiescent absolute magnitude of an object 3–4 mag brighter than that of ordinary short-period systems, as shown in figure 2 of Paper I. Our proposed scenario can thus reconcile the problems of this object against the standard evolutionary sequence of CVs.

This scenario predicts that the binary system shrinks with time until the secondary star degenerates. At the period minimum, the surface abundance of hydrogen will significantly decrease compared with the current state. The object, hence, possibly appears to be an AM CVn star after the period minimum. This is just the CV channel proposed as an evolutionary sequence of AM CVn stars by Podsiadlowski et al. (2001). Marsh and Steeghs (2002) have recently suggested that V407 Vul, which is proposed to be a binary system with a 9.5-min orbital period, is a progenitor of AM CVn stars on the course of the white-dwarf channel. The present discovery of a high $\dot{M}$ and a luminous secondary star of 1RXS J232953.9+062814 provides stronger observational support for the CV channel to be an evolutionary sequence of AM CVn stars.

4. Summary

Our detailed analysis of short-term modulations revealed the evolution of superhumps and late superhumps observed in 1RXS J232953.9+062814. Superhumps appeared during the main plateau, rapid fading and rebrightening phase. They then disappeared during the transition phase. The superhump period increased with time at a relatively large rate during the main plateau phase. The period increase was interrupted when the object entered the rapid fading phase. During the rebrightening phase and the transition phase, the superhump period continued to decrease. The period increase, the rebrightening, and the long fading tail are characteristics observed in WZ Sge stars or short-period SU UMa stars, although 1RXS J232953.9+062814 has a large mass ratio and accretion rate. Late superhumps subsequently appeared since the early post-outburst phase. They were long-lived and showed no significant systematic period change. We propose a possible evolutionary scenario of this object that it is a progenitor of AM CVn stars on the course of the CV channel.

We are pleased to acknowledge comments by D. Nogami, and vital observations via VSNET by many amateur observers. Part of this work is supported by a Research Fellowship of the Japan Society for the Promotion of Science for Young Scientists (MU). This work is partly supported by a grant-in-aid (13640239) from the Ministry of Education, Culture, Sports, Science and Technology.

References

Baraffe, I., & Kolb, U. 2000, MNRAS, 318, 354
Haefner, R., Schoembs, R., & Vogt, N. 1979, A&A, 77, 7
Iben, I., Jr. & Tutukov, A. V. 1991, ApJ, 370, 615
Kato, T., Nogami, D., Matsumoto, K., & Baba, H. 1997, ⟨ftp://ftp.kusastro.kyoto-u.ac.jp/pub/vsnet/preprints/EG_Cnc/⟩
Kato, T., Sekine, Y., & Hirata, R. 2001, PASJ, 53, 1191
King, A. R. 1988, QJRAS, 29, 1
Marsh, T. R., & Steeghs, D. 2002, MNRAS, 331, L7
Nelemans, G., Steeghs, D., & Groot, P. J. 2001, MNRAS, 326, 621
Olech, A. 1997, Acta Astron., 47, 281
Osaki, Y. 1995, PASJ, 47, 47
Osaki, Y. 1996, PASP, 108, 39
Osaki, Y., Meyer, F., & Meyer-Hofmeister, E. 2001, A&A, 370, 488
Osaki, Y., Shimizu, S., & Tsugawa, M. 1997, PASJ, 49, L19
Paczyński, B. 1981, Acta Astron., 31, 1
Patterson, J., Bond, H. E., Grauer, A. D., Shafter, A. W., & Mattei, J. A. 1993, PASP, 105, 69
Podsiadlowski, P., Han, Z., & Rappaport, S. 2001, MNRAS, submitted (astro-ph/0109171)
Rappaport, S., Verbunt, F., & Joss, P. C. 1983, ApJ, 275, 713
Smak, J. 1967, Acta Astron., 17, 255
Sproats, L. N., Howell, S. B., & Mason, K. O. 1996, MNRAS, 282, 1211
Stellingwerf, R. F. 1978, ApJ, 224, 953
Taam, R. E., Flannery, B. P., & Faulkner, J. 1980, ApJ, 239, 1017
Thorstensen, J. R., Fenton, W. H., Patterson, J. O., Kemp, J., Krajci, T., & Baraffe, I. 2002, ApJ, 567, L49
Tutukov, A. V., & Yungelson, L. R. 1979, Acta Astron., 29, 665
Uemura, M., Ishioka, R., Kato, T., Schmeer, P., Yamaoka, H., Starkey, D., Vanmunster, T., & Pietz, J. 2001, IAU Circ., 7747
Uemura, M., Kato, T., Ishioka, R., Yamaoka, H., Schmeer, P., Starkey, D. R., Torii, K., Kawai, N., et al. 2002, PASJ, 54, L15 (Paper I)
Vogt, N. 1983, A&A, 118, 95
Warner, B. 1985, in Interacting Binaries, ed. P. P. Eggleton & J. E. Pringle (Dordrecht: D. Reidel Publishing Company), 367
Warner, B. 1987, Ap&SS, 130, 3
Warner, B. 1995, Cataclysmic Variable Stars (Cambridge: Cambridge University Press)
Warner, B., & Robinson, E. L. 1972, MNRAS, 159, 101